

Reversible aryl C–H bond activation in the reaction between $\text{HRu}_3(\text{CO})_{9,10}(\mu\text{-PPh}_2)$ and the diphosphine ligand 4,5-bis(diphenylphosphino)-4-cyclopenten-1,3-dione (bpcd): X-ray diffraction structures of $\text{H}_2\text{Ru}_3(\text{CO})_7(\text{bpcd})[\mu, \sigma\text{-PPh}(\text{C}_6\text{H}_4)]$ and $\text{Ru}_3(\text{CO})_6(\mu\text{-CO})(\mu\text{-PPh}_2)[\mu, \eta^2, \eta^1\text{-PPhC}=\text{C}(\text{PPh}_2)\text{C}(\text{O})\text{CH}_2\text{C}(\text{O})]$

Simon G. Bott ^{a,*}, Huafeng Shen ^b, Michael G. Richmond ^{b,*}

^a Department of Chemistry, University of Houston, Houston, TX 77204, USA

^b Department of Chemistry, University of North Texas, Denton, TX 76203, USA

Received 1 March 2005; received in revised form 17 May 2005; accepted 17 May 2005

Available online 12 July 2005

Abstract

The reaction between $\text{HRu}_3(\text{CO})_{10}(\mu\text{-PPh}_2)$ (**1**) and the diphosphine ligand 4,5-bis(diphenylphosphino)-4-cyclopenten-1,3-dione (bpcd) proceeds rapidly in the presence of Me_3NO to furnish $\text{H}_2\text{Ru}_3(\text{CO})_7(\text{bpcd})[\mu, \sigma\text{-PPh}(\text{C}_6\text{H}_4)]$ (**3**). Treatment of the nonacarbonyl cluster $\text{HRu}_3(\text{CO})_9(\mu\text{-PPh}_2)$ (**2**) with bpcd at room temperature affords cluster **3** as the major product in addition to cluster **1**. Thermolysis of cluster **3** in 1,2-dichloroethane yields $\text{Ru}_3(\text{CO})_6(\mu\text{-CO})(\mu\text{-PPh}_2)[\mu, \eta^2, \eta^1\text{-PPhC}=\text{C}(\text{PPh}_2)\text{C}(\text{O})\text{CH}_2\text{C}(\text{O})]$ (**4**) as the major isolable product. The highlights associated with the production of cluster **4** involve the reductive elimination of the orthometalated aryl group with one of the two bridging hydrides in **3** and cleavage of one of the P–Ph bonds of the bpcd ligand, followed by the release of benzene from the transient sigma-bound Ru–Ph group. Both $\text{H}_2\text{Ru}_3(\text{CO})_7(\text{bpcd})[\mu, \sigma\text{-PPh}(\text{C}_6\text{H}_4)]$ and $\text{Ru}_3(\text{CO})_6(\mu\text{-CO})(\mu\text{-PPh}_2)[\mu, \eta^2, \eta^1\text{-PPhC}=\text{C}(\text{PPh}_2)\text{C}(\text{O})\text{CH}_2\text{C}(\text{O})]$ have been isolated and characterized in solution by IR and NMR (³¹P and ¹H) spectroscopies, in addition to X-ray crystallography. The solid-state structure of $\text{H}_2\text{Ru}_3(\text{CO})_7(\text{bpcd})[\mu, \sigma\text{-PPh}(\text{C}_6\text{H}_4)]$ confirms the presence of an orthometalated μ_2 -phosphido moiety and a chelating bpcd ligand. The crystal structure of cluster **4** consists of a triangular Ru_3 core where one face is capped by the 6e-donor ligand $\mu, \eta^2, \eta^1\text{-PPhC}=\text{C}(\text{PPh}_2)\text{C}(\text{O})\text{CH}_2\text{C}(\text{O})$. © 2005 Elsevier B.V. All rights reserved.

Keywords: Ruthenium cluster; Phosphido compounds; Orthometalation; Diphosphine ligand

1. Introduction

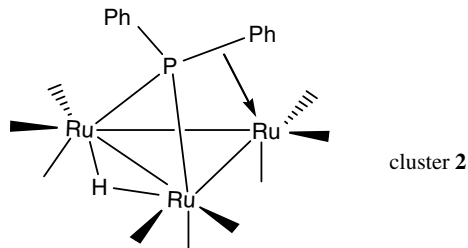
The reactivity of the triruthenium clusters $\text{HRu}_3(\text{CO})_{10}(\mu\text{-PPh}_2)$ (**1**) and $\text{HRu}_3(\text{CO})_9(\mu\text{-PPh}_2)$ (**2**) in ligand substitution reactions and catalytic hydrogenations has been extensively explored [1–5]. The latter clus-

ter, which is readily obtained from the Me_3NO -promoted decarbonylation of $\text{HRu}_3(\text{CO})_{10}(\mu\text{-PPh}_2)$ [6] or by hydrogenation of the acetylide-bridged clusters $\text{Ru}_3(\text{CO})_8(\mu_3\text{-}\eta^2\text{-CCR})(\mu_2\text{-PPh}_2)$ (where $\text{R} = \text{Bu}^t, \text{Pr}^i$) [7], has invoked considerable interest due to its formal unsaturation that is alleviated by coordination of one of the two P–Ph bonds to the non-hydride-bridged Ru center, as shown below [8]. Such an η^2 -coordination of the P–Ph bond is akin to an agostic interaction between a metal and an alkane [9] and may be viewed as an arrested or precursor state for the oxidative cleavage of

* Corresponding authors. Tel.: +1 713 743 2771 (S.G. Bott), Tel.: +1 940 565 3548; fax: +1 940 565 4318 (M.G. Richmond).

E-mail addresses: sbott@uh.edu (S.G. Bott), cobalt@unt.edu (M.G. Richmond).

P–Ph bonds at a transition-metal center [10]. The facile addition of a variety of substrates to $\text{HRu}_3(\text{CO})_9(\mu\text{-PPh}_2)$ (**2**) suggests that the P–Ph bond is weakly bound to the ruthenium center and that its dissociation provides a low-energy pathway for the generation of a coordinatively unsaturated site within the cluster [3].



Recently, we have published our results on the ligand substitution behavior of the azavinylidene-bridged cluster $\text{HRu}_3(\text{CO})_{10}(\mu\text{-NCPH}_2)$ with the diphosphine ligands 1,2-bis(dimethylphosphino)ethane (dmpe) and 4,5-bis(diphenylphosphino)-4-cyclopenten-1,3-dione (bpcd), with the coordination of these ligands giving bridged and chelated diphosphine-substituted clusters, respectively, as depicted in Scheme 1 [11]. $\text{HRu}_3(\text{CO})_{10}(\mu\text{-NCPH}_2)$ is structurally similar to the triruthenium clusters $\text{HRu}_3(\text{CO})_{10}(\mu\text{-PPh}_2)$ (**1**) and $\text{HRu}_3(\text{CO})_9(\mu\text{-PPh}_2)$ (**2**), inasmuch as it possesses a hydride- and pnictogen-bridged ruthenium–ruthenium bond, and this structural similarity, coupled with the absence of reports for the reaction of clusters **1** and **2** with diphosphine ligands,

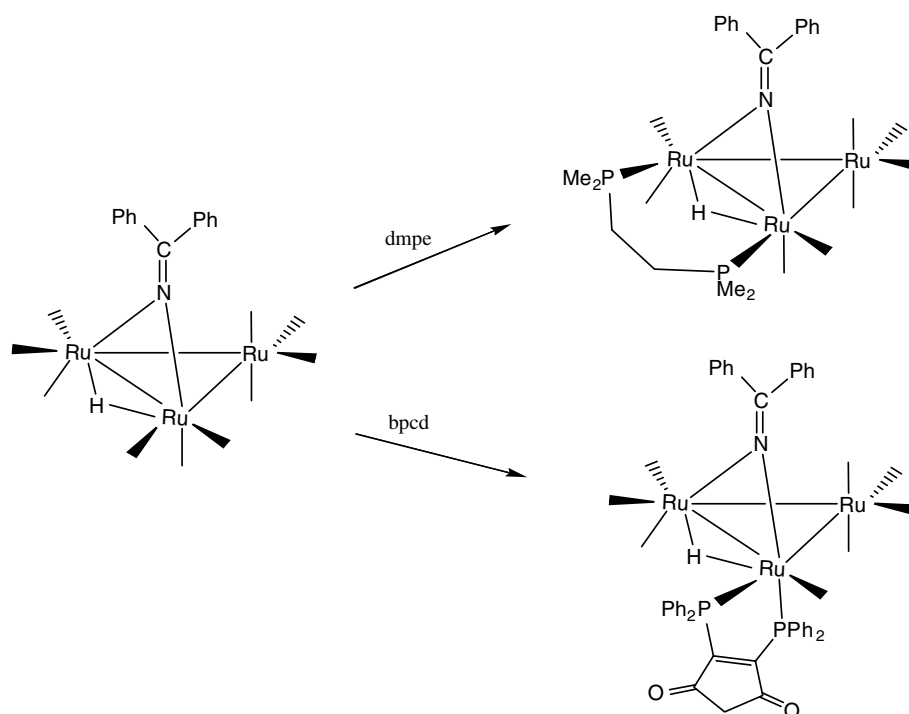
would allow us to test the generality associated with the mode of diphosphine coordination in a given polyhedral motif.

With this rationale for our interest in $\text{HRu}_3(\text{CO})_{10}(\mu\text{-PPh}_2)$ (**1**) and $\text{HRu}_3(\text{CO})_9(\mu\text{-PPh}_2)$ (**2**), we have studied the reaction between clusters **1** and **2** with the diphosphine ligand bpcd [12]. Herein, we present our data on synthesis and structural characterization of the new clusters $\text{H}_2\text{Ru}_3(\text{CO})_7(\text{bpcd})[\mu, \sigma\text{-PPh}(\text{C}_6\text{H}_4)]$ (**3**) and $\text{Ru}_3(\text{CO})_6(\mu\text{-CO})(\mu\text{-PPh}_2)[\mu, \eta^2, \eta^1\text{-PPhC}=\text{C}(\text{PPh}_2)\text{C}(\text{O})\text{-CH}_2\text{C}(\text{O})]$ (**4**). Controlled thermolysis reactions establish cluster **3** as the precursor to cluster **4**. Chelation of the bpcd ligand to the cluster polyhedron is accompanied by an orthometalation of one the aryl groups belonging to the bridging phosphido moiety and this C–H bond activation is reversed upon thermolysis of cluster **3**. The reformation of the $\mu\text{-PPh}_2$ moiety in cluster **4** is accompanied by P–Ph activation of the ancillary bpcd ligand and release of benzene.

2. Experimental

2.1. General methods

The $\text{Ru}_3(\text{CO})_{12}$ and bpcd ligand used in these studies were synthesized from hydrated RuCl_3 and 4,5-dichloro-4-cyclopenten-1,3-dione, respectively, according to known procedures [13,14]. All reaction and NMR solvents were distilled under argon from a suitable



Scheme 1.

drying agent and stored in Schlenk storage vessels [15]. The combustion analyses were performed by Altantic Microlab, Norcross, GA.

The reported infrared data were recorded on a Nicolet 20 SXB FT-IR spectrometer in 0.1 mm amalgamated NaCl cells, using PC control and OMNIC software, while the ^1H NMR spectra were recorded at 200 MHz on a Varian Gemini-200 spectrometer. The ^{31}P NMR spectra were recorded at 121 MHz on a Varian 300-VXR spectrometer in the proton-decoupled mode, with the reported ^{31}P chemical shifts being referenced to external H_3PO_4 (85%), taken to have $\delta = 0.0$. Here positive chemical shifts are to low field of the external standard.

2.2. Synthesis of $\text{H}_2\text{Ru}_3(\text{CO})_7(\text{bpcd})[\mu, \sigma\text{-PPh}(\text{C}_6\text{H}_4)]$ from $\text{HRu}_3(\text{CO})_{9,10}(\mu\text{-PPh}_2)$ and *bpcd*

2.2.1. From $\text{HRu}_3(\text{CO})_{10}(\mu\text{-PPh}_2)$ and Me_3NO

To 0.10 g (0.13 mmol) of $\text{HRu}_3(\text{CO})_{10}(\mu\text{-PPh}_2)$ (**1**) and 60 mg (0.13 mmol) of *bpcd* in a Schlenk tube under argon was added 30 mL of CH_2Cl_2 , followed by 20 mg (0.27 mmol) of Me_3NO . The reaction solution immediately changed from yellow to red in color, with stirring continued for an additional 1.0 h at room temperature. TLC analysis using CH_2Cl_2 /petroleum ether (1:1) revealed the presence of a small amount of cluster **1** ($R_f = 0.90$) and a red spot ($R_f = 0.45$) corresponding to $\text{H}_2\text{Ru}_3(\text{CO})_7(\text{bpcd})[\mu, \sigma\text{-PPh}(\text{C}_6\text{H}_4)]$ (**3**), along with some material that remained at the origin of the TLC plate. The reaction solvent was removed under vacuum and the crude mixture was separated by column chromatography over silica gel. Use of petroleum ether as the eluent afforded cluster **1**, after which CH_2Cl_2 was employed as the mobile phase for the elution of pure **3**. Single crystals of $\text{H}_2\text{Ru}_3(\text{CO})_7(\text{bpcd})[\mu, \sigma\text{-PPh}(\text{C}_6\text{H}_4)]$ suitable for combustion analysis and X-ray diffraction examination were grown from a toluene solution containing cluster **3** that had been layered with pentane. Yield of red **3**: 85 mg (57%). IR (CH_2Cl_2): $\nu(\text{CO})$ 2057 (s), 2033 (m), 2019 (s), 2000 (s), 1984 (sh), 1963 (sh), 1929 (sh), 1749 (m, *symm* dione carbonyl), 1717 (s, *antisymm* dione carbonyl) cm^{-1} . ^1H NMR (CDCl_3): δ 8.00–6.15 (29H, aromatics), 3.66 (2H, AB quartet, $^2J_{\text{H-H}} = 22$ Hz), –13.44 (1H, multiplet), –17.14 (1H, quartet, $J = 12$ Hz). $^{31}\text{P}\{^1\text{H}\}$ NMR (CDCl_3): δ 121.19 ($\mu_2\text{-PPh}_2$, dd, $^2J_{\text{P-P}} = 194$, 13 Hz), 48.30 (broad triplet, $^2J_{\text{P-P}} = \text{ca. } 14$ Hz), 47.01 (dd, $^2J_{\text{P-P}} = 194$, 13 Hz). Anal. Calcd (found) for $\text{C}_{48}\text{H}_{33}\text{O}_9\text{P}_3\text{Ru}_3 \cdot \text{toluene}$: C, 53.19 (53.27); H, 3.33 (4.02).

2.2.2. From the direct reaction with $\text{HRu}_3(\text{CO})_9(\mu\text{-PPh}_2)$

To 0.10 g (0.13 mmol) of $\text{HRu}_3(\text{CO})_9(\mu\text{-PPh}_2)$ (**2**) in 25 mL of CH_2Cl_2 was added 60 mg (0.13 mmol) of *bpcd*. As before, the reaction solution immediately changed in color from yellow to red, supporting the formation of

cluster **3**. The reaction was stirred for 0.5 h and then examined by TLC analysis, which confirmed the presence of $\text{H}_2\text{Ru}_3(\text{CO})_7(\text{bpcd})[\mu, \sigma\text{-PPh}(\text{C}_6\text{H}_4)]$ as the major product, along with the formation of a trace amount of cluster **1**. Both products were isolated as described above. Yield of **3**: 0.11 g (73%).

2.3. Thermolysis of $\text{H}_2\text{Ru}_3(\text{CO})_7(\text{bpcd})[\mu, \sigma\text{-PPh}(\text{C}_6\text{H}_4)]$ to $\text{Ru}_3(\text{CO})_6(\mu\text{-CO})(\mu\text{-PPh}_2)[\mu, \eta^2, \eta^1\text{-PPhC}=\text{C}(\text{PPh}_2)\text{C}(\text{O})\text{CH}_2\text{C}(\text{O})]$

To a small Schlenk vessel containing 0.10 g (0.087 mmol) of $\text{H}_2\text{Ru}_3(\text{CO})_7(\text{bpcd})[\mu, \sigma\text{-PPh}(\text{C}_6\text{H}_4)]$ under argon was added 25 mL of 1,2-dichloroethane, after which the vessel was heated at ca. 80 °C for 2.0 h. The reaction was allowed to cool to room temperature and was examined by TLC analysis (CH_2Cl_2), which revealed the presence of a trace amount of a fast moving yellow spot ($R_f = 0.85$), a purple spot ($R_f = 0.25$), and extensive decomposition, as evidenced by the large amount of black-colored material that remained at the origin. Cluster **4** was isolated by column chromatography over silica gel using CH_2Cl_2 and was recrystallized from a 1:1 mixture of CH_2Cl_2 /pentane. Yield of **4**: 33 mg (22%). IR (CH_2Cl_2): $\nu(\text{CO})$ 2049 (m), 2021 (vs), 1995 (s), 1950 (sh), 1892 (m), 1716 (m, *symm* dione carbonyl), 1684 (m, *antisymm* dione carbonyl) cm^{-1} . ^1H NMR (CDCl_3): δ 8.00–6.60 (25H, aromatics), 3.54 (2H, AB quartet, $^2J_{\text{H-H}} = 22$ Hz). $^{31}\text{P}\{^1\text{H}\}$ NMR (CDCl_3): δ 249.97 ($\mu_2\text{-phosphido}$, dd, $^2J_{\text{P-P}} = 171$, 79 Hz), 64.60 ($\mu_2\text{-phosphido}$, dd, $^2J_{\text{P-P}} = 79$, 18 Hz), 6.14 (phosphine, dd, $^2J_{\text{P-P}} = 171$, 18 Hz). Anal. Calcd (found) for $\text{C}_{46}\text{H}_{27}\text{O}_9\text{P}_3\text{Ru}_3 \cdot 1/2\text{CH}_2\text{Cl}_2$: C, 47.079 (46.81); H, 2.54 (2.63).

2.4. X-ray crystallography for clusters **3** and **4**

Selected crystals of $\text{H}_2\text{Ru}_3(\text{CO})_7(\text{bpcd})[\mu, \sigma\text{-PPh}(\text{C}_6\text{H}_4)]$ and $\text{Ru}_3(\text{CO})_6(\mu\text{-CO})(\mu\text{-PPh}_2)[\mu, \eta^2, \eta^1\text{-PPhC}=\text{C}(\text{PPh}_2)\text{C}(\text{O})\text{CH}_2\text{C}(\text{O})]$ suitable for X-ray diffraction analysis were grown as described above and were each sealed inside a Lindemann capillary, followed by mounting on an Enraf-Nonius CAD-4 diffractometer. After the cell constants were obtained for both samples, intensity data in the range of $2^\circ \leq 2\theta \leq 44^\circ$ were collected at 298 K and were corrected for Lorentz, polarization, and absorption (DIFABS). The structures were solved by using SHELX-86 (cluster **3**) and Multan (cluster **4**). All non-hydrogen atoms were located with difference Fourier maps and full-matrix least-squares refinement and were refined anisotropically with the exception of the carbon and oxygen groups in cluster **3**. Due to the unresolved disorder and paucity of data, the bridging hydride atoms in **3** could not be located. All non-hydrogen atoms in cluster **4** were refined anisotropically with the exception of the ancillary phenyl carbons. Refinement

on **3** converged at $R = 0.0613$ and $R_w = 0.0731$ for 5191 unique reflections with $I > 3\sigma(I)$, while for **4** refinement converged at $R = 0.0438$ and $R_w = 0.0503$ for 4192 unique reflections with $I > 3\sigma(I)$.

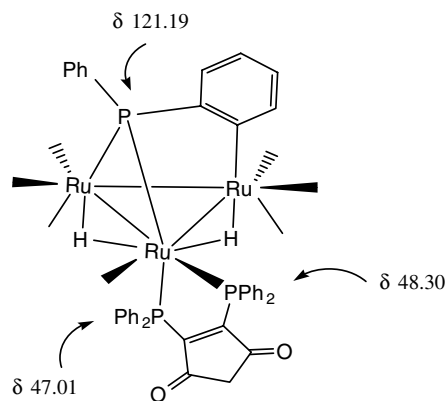
3. Results and discussion

3.1. Syntheses, spectroscopic data, and X-ray diffraction structure for $H_2Ru_3(CO)_7(bpcd)[\mu, \sigma-PPh(C_6H_4)]$

Treatment of the saturated cluster $HRu_3(CO)_{10}(\mu-PPh_2)$ (**1**) and bpcd at room temperature in CH_2Cl_2 with two equivalents of Me_3NO leads to a rapid production of the new cluster $H_2Ru_3(CO)_7(bpcd)[\mu, \sigma-PPh(C_6H_4)]$ (**3**) as the major product. No reaction between **1** and bpcd was observed in the absence of Me_3NO , and while heating a 1,2-dichloroethane solution containing $HRu_3(CO)_{10}(\mu-PPh_2)$ and bpcd at $80^\circ C$ did show TLC evidence for the formation of the desired product **3** and a purple spot, that was later confirmed as $Ru_3(CO)_6(\mu-CO)(\mu-PPh_2)[\mu, \eta^2, \eta^1-PPhC=C(PPh_2)C(O)CH_2C(O)]$, there was considerable decomposition observed, rendering this method of little synthetic value in the preparation of cluster **3**. $H_2Ru_3(CO)_7(bpcd)[\mu, \sigma-PPh(C_6H_4)]$ has also been obtained from the direct reaction of the reactive, 46-electron cluster $HRu_3(CO)_9(\mu-PPh_2)$ (**2**) with bpcd. In the case of the reaction employing cluster **2** as a starting material, the small amount of $HRu_3(CO)_{10}(\mu-PPh_2)$ that always accompanies the production of cluster **3** derives from the capture of the liberated CO by $HRu_3(CO)_9(\mu-PPh_2)$ [2,7]. TLC analyses revealed that these reactions giving cluster **3** were essentially complete after several minutes, but as a matter of protocol we typically allowed the reaction to be stirred for short period of time (ca. 1.0 h) before chromatographic separation over silica gel. $H_2Ru_3(CO)_7(bpcd)[\mu, \sigma-PPh(C_6H_4)]$ was isolated as a red solid that was found to be stable in the solid state under argon for several weeks. Solutions of **3** exposed to oxygen are less stable, showing signs of slow decomposition over the course of several hours.

Cluster **3** was characterized in solution by standard methods. Terminal carbonyl stretching bands from 2057 to 1929 cm^{-1} were found for the ruthenium-bound CO groups, with the $\nu(CO)$ bands at 1749 and 1717 cm^{-1} ascribed to the vibrationally coupled symmetric and antisymmetric dione $C=O$ stretches, respectively [16]. The 1H NMR spectral highlights include an AB quartet centered at δ 3.66 for the diastereotopic hydrogens associated with the dione ring of the ancillary bpcd ligand and two, high-field bridging hydrides at δ -13.44 and -17.14 that are coupled to all three phosphorus centers. The ^{31}P NMR spectrum of **3** reveals the presence of three resonances at δ 47.01, 48.30, and

121.19. Here, the latter down field resonance is readily to a μ_2 -phosphido moiety, with the remaining two ^{31}P chemical shifts consistent with a chelated bpcd ligand [17]. The unequivocal ^{31}P assignments for cluster **3**, taken in conjunction with the solid-state structure (vide infra), are shown below.



The molecular structure of cluster **3** was established by X-ray crystallography. Single crystals of **3** crystallize in the unit cell as two independent molecules with no unusually short inter- or intramolecular contacts. Tables 1 and 2 report the X-ray data collection and processing parameters and selected bond distances and angles, respectively.

Table 1

X-ray crystallographic data and processing parameters for the triruthenium clusters $H_2Ru_3(CO)_7(bpcd)[\mu, \sigma-PPh(C_6H_4)]$ (**3**) and $Ru_3(CO)_6(\mu-CO)(\mu-PPh_2)[\mu, \eta^2, \eta^1-PPhC=C(PPh_2)C(O)CH_2C(O)]$ (**4**)

	Compound 3	Compound 4
CCDC entry no.	264527	264526
Space group	Triclinic, $P\bar{1}$	Triclinic, $P\bar{1}$
a (Å)	11.335(2)	12.2894(7)
b (Å)	20.111(3)	14.505(1)
c (Å)	22.818(2)	14.798(1)
α (°)	68.28(1)	104.418(8)
β (°)	83.07(1)	113.749(6)
γ (°)	86.50(1)	101.695(6)
V (Å ³)	4796(1)	2197.6(4)
Molecular formula	$C_{48}H_{33}O_9P_3Ru_3 \cdot 1/4\text{toluene}$	$C_{42}H_{27}O_9P_3Ru_3 \cdot CH_2Cl_2$
fw	1171.96	1156.74
Formula units per cell (Z)	4	2
D_{calcd} ($g\text{ cm}^{-3}$)	1.622	1.748
λ (Mo $K\alpha$) (Å)	0.71073	0.71073
Absorption coefficient (cm^{-1})	10.66	12.81
Abs corr factor	0.87–1.13	0.82–1.17
Total reflections	11716	5366
Independent reflections	5191	4192
Data/res/parameters	5191/0/577	4192/0/391
R	0.0613	0.0438
R_w	0.0731	0.0503
GOF on F^2	0.88	1.12
Weights	$[0.04F^2 + (\sigma F)^2]^{-1}$	$[0.04F^2 + (\sigma F)^2]^{-1}$

Table 2

Selected bond distances (Å) and angles (°) in the triruthenium clusters $\text{H}_2\text{Ru}_3(\text{CO})_7(\text{bpcd})[\mu, \sigma\text{-PPh}(\text{C}_6\text{H}_4)]$ and $\text{Ru}_3(\text{CO})_6(\mu\text{-CO})(\mu\text{-PPh}_2)[\mu, \eta^2, \eta^1\text{-PPhC}=\text{C}(\text{PPh}_2)\text{C}(\text{O})\text{CH}_2\text{C}(\text{O})]^\text{a}$

Molecule A		Molecule B	
$\text{H}_2\text{Ru}_3(\text{CO})_7(\text{bpcd})[\mu, \sigma\text{-PPh}(\text{C}_6\text{H}_4)]$			
<i>Bond distances</i>			
Ru(1a)–Ru(2a)	2.910(2)	Ru(1b)–Ru(2b)	2.940(3)
Ru(1a)–Ru(3a)	3.075(2)	Ru(1b)–Ru(3b)	3.065(3)
Ru(2a)–Ru(3a)	2.820(2)	Ru(2b)–Ru(3b)	2.839(3)
Ru(1a)–P(1a)	2.312(5)	Ru(1b)–P(1b)	2.300(6)
Ru(1a)–P(2a)	2.337(6)	Ru(1b)–P(2b)	2.359(5)
Ru(1a)–P(3a)	2.328(6)	Ru(1b)–P(3b)	2.308(5)
Ru(2a)–P(3a)	2.325(5)	Ru(2b)–P(3b)	2.332(6)
Ru(3a)–C(312a)	2.15(2)	Ru(3b)–C(312b)	2.14(2)
C(11a)–C(15A)	1.33(3)	C(11b)–C(15b)	1.36(2)
<i>Bond angles</i>			
P(1a)–Ru(1a)–P(2a)	85.2(2)	P(1b)–Ru(1b)–P(2b)	86.5(2)
P(1a)–Ru(1a)–P(3a)	107.2(2)	P(1b)–Ru(1b)–P(3b)	101.5(2)
P(1a)–Ru(1a)–C(1a)	90.4(6)	P(1b)–Ru(1b)–C(1b)	94.6(7)
P(2a)–Ru(1a)–P(3a)	167.3(2)	P(2b)–Ru(1b)–P(3b)	171.2(2)
P(2a)–Ru(1a)–C(1a)	89.4(8)	P(2b)–Ru(1b)–C(1b)	91.7(6)
P(3a)–Ru(1a)–C(1a)	93.3(8)	P(3b)–Ru(1b)–C(1b)	91.4(6)
Ru(1a)–Ru(3a)–C(312a)	91.1(5)	Ru(1b)–Ru(3b)–C(312b)	89.7(6)
Ru(2a)–Ru(3a)–C(312a)	91.7(5)	Ru(2b)–Ru(3b)–C(312b)	90.2(5)
C(5a)–Ru(3a)–C(312a)	179.3(8)	C(5b)–Ru(3b)–C(312b)	89.5(8)
$\text{Ru}_3(\text{CO})_6(\mu\text{-CO})(\mu\text{-PPh}_2)[\mu, \eta^2, \eta^1\text{-PPhC}=\text{C}(\text{PPh}_2)\text{C}(\text{O})\text{CH}_2\text{C}(\text{O})]$			
<i>Bond distances</i>			
Ru(1)–Ru(2)	2.901(1)	Ru(1)–Ru(3)	2.981(1)
Ru(2)–Ru(3)	2.742(1)	Ru(1)–P(1)	2.375(3)
Ru(1)–P(2)	2.340(2)	Ru(1)–P(3)	2.375(3)
Ru(2)–P(2)	2.337(3)	Ru(2)–P(3)	2.308(2)
Ru(2)–C(5)	2.133(8)	Ru(3)–C(5)	2.13(1)
Ru(3)–C(11)	2.19(1)	Ru(3)–C(15)	2.198(8)
C(11)–C(15)	1.41(1)		
<i>Bond angles</i>			
P(1)–Ru(1)–P(2)	84.67(8)	P(1)–Ru(1)–P(3)	164.86(6)
P(2)–Ru(1)–P(3)	80.22(8)	P(2)–Ru(2)–P(3)	81.70(8)
C(11)–Ru(3)–C(15)	37.6(3)	Ru(1)–P(2)–Ru(2)	76.69(6)
Ru(1)–P(3)–Ru(2)	76.55(8)	Ru(2)–C(5)–Ru(3)	80.2(3)
Ru(2)–C(5)–O(5)	143.3(8)	Ru(3)–C(5)–O(5)	136.0(8)
Ru(3)–C(11)–P(1)	96.3(3)	Ru(3)–C(15)–P(2)	90.4(3)

^a Numbers in parentheses are estimated standard deviations in the least significant digits.

The ORTEP diagram of one of the independent molecules of $\text{H}_2\text{Ru}_3(\text{CO})_7(\text{bpcd})[\mu, \sigma\text{-PPh}(\text{C}_6\text{H}_4)]$ (**3**) is shown in Fig. 1. Since the two molecules of $\text{H}_2\text{Ru}_3(\text{CO})_7(\text{bpcd})[\mu, \sigma\text{-PPh}(\text{C}_6\text{H}_4)]$ (A and B) show only minor structural differences, we will present and discuss the highlights of only molecule A. The two most important structural features found for this 48-electron cluster include the chelation of the bpcd ligand to the Ru(1a) center and the orthometalation of one of the phenyl groups associated with the original $\mu_2\text{-PPh}_2$ moiety in clusters **1** and **2**. This orthometalation leads to a Ru(3a)–C(312a) sigma bond of 2.15(2) Å, whose distance is in good agreement with related orthometalated cluster $[\text{HRu}_3(\text{CO})_8(\text{PPh}_3)\{\mu, \sigma\text{-PPh}(\text{C}_6\text{H}_4)\}]^-$ [18] and other structurally characterized compounds possessing an orthometalated Ru–C(aryl) bond [19]. This activated phenyl group [atoms C(311a)–C(316a)] is orthogonally disposed to

the plane defined by the three ruthenium atoms, on the basis of a dihedral angle of 91°. The Ru–Ru bond lengths, while distinctly asymmetric in nature given the bond distances of 3.075(2) Å [Ru(1a)–Ru(3a)], 2.910(2) Å [Ru(1a)–Ru(2a)], and 2.820(3) Å [Ru(2a)–Ru(3a)], are in excellent agreement with values reported for other Ru_3 cluster compounds [20]. Despite the fact that the positions of the two bridging hydride ligands were not crystallographically found, we have assigned them to the longer Ru(1a)–Ru(3a) and Ru(1a)–Ru(2a) bonds in keeping with the generally recognized trend of hydrido-bridged metal–metal bonds being longer than non-hydrido-bridged metal–metal bonds [21]. The Ru–P distances range from 2.312(5) Å [Ru(1a)–P(1a)] to 2.337(6) Å [Ru(1a)–P(2a)] with an average distance of 2.326 Å. The arrangement of the three phosphorus centers attached to Ru(1a) corroborate the ³¹P spectral

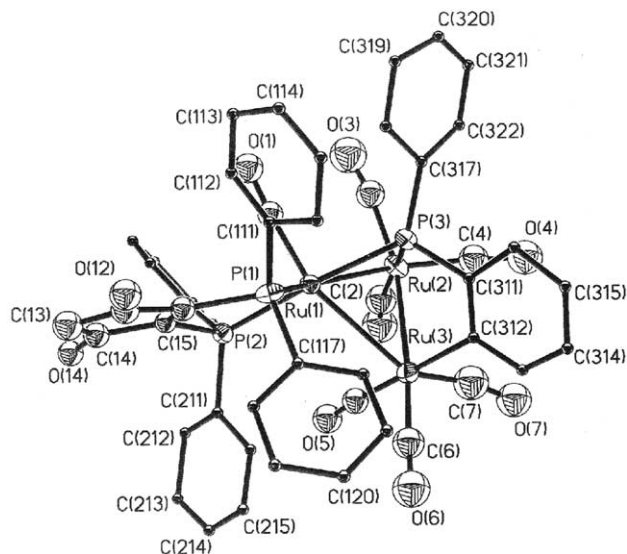


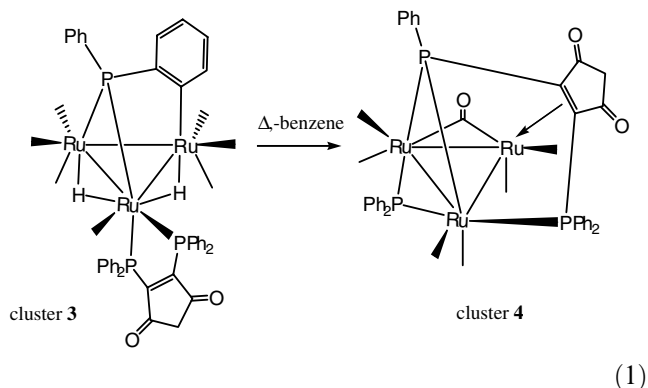
Fig. 1. ORTEP drawing of one of the two independent molecules of $\text{H}_2\text{Ru}_3(\text{CO})_7(\text{bpcd})[\mu, \sigma\text{-PPh}(\text{C}_6\text{H}_4)]$ showing the thermal ellipsoids at the 50% probability level.

assignments for cluster **3**. The P(1a) atom is mutually *cis* to the P(2a) and P(3a) centers, on the basis of P(1a)–Ru(1a)–P(2a) and P(1a)–Ru(1a)–P(3a) angles of $85.2(2)^\circ$ and $107.2(2)^\circ$, respectively, and is expected to give a ^{31}P triplet resonance with small P–P coupling. The nearly *trans* orientation found for the P(2a)–Ru(1a)–P(3a) linkage is verified by an angle of $167.3(2)^\circ$. The seven carbonyl groups found in **3** are linear and exhibit bond distances typical for ruthenium carbonyl units. The C(11a)–C(15a) carbon–carbon double bond length of $1.32(2) \text{ \AA}$ in the dione ring is in good agreement with the C=C bond distance of simple alkenes and the analogous bond distance in bpcd-substituted complexes prepared by us [22]. The remaining bond distances and angles are unexceptional and do not require comment.

3.2. Thermal stability of $\text{H}_2\text{Ru}_3(\text{CO})_7(\text{bpcd})[\mu, \sigma\text{-PPh}(\text{C}_6\text{H}_4)]$: synthesis, spectroscopic data, and X-ray diffraction structure for $\text{Ru}_3(\text{CO})_6(\mu\text{-CO})(\mu\text{-PPh}_2)[\mu, \eta^2, \eta^1\text{-PPhC}=\text{C}(\text{PPh}_2)\text{C}(\text{O})\text{CH}_2\text{C}(\text{O})]$

The thermal reactivity of $\text{H}_2\text{Ru}_3(\text{CO})_7(\text{bpcd})[\mu, \sigma\text{-PPh}(\text{C}_6\text{H}_4)]$ was next explored due to the less than straightforward reaction between $\text{HRu}_3(\text{CO})_{10}(\mu\text{-PPh}_2)$ and bpcd (vide supra). Heating $\text{H}_2\text{Ru}_3(\text{CO})_7(\text{bpcd})[\mu, \sigma\text{-PPh}(\text{C}_6\text{H}_4)]$ in DCE at 80°C under argon led to the rapid consumption of cluster **3** and the simultaneous formation of a purple spot and extensive decomposition, as assessed by TLC examination of the reaction solution. The purple compound, whose identity was later determined as $\text{Ru}_3(\text{CO})_6(\mu\text{-CO})(\mu\text{-PPh}_2)[\mu, \eta^2, \eta^1\text{-PPhC}=\text{C}(\text{PPh}_2)\text{C}(\text{O})\text{CH}_2\text{C}(\text{O})]$ (**4**), was subsequently isolated by column chromatography over silica

gel and characterized in solution by IR and NMR spectroscopies. Eq. (1) shows the reaction between **3** and **4**.



Cluster **4** displays terminal $\nu(\text{CO})$ bands at 2049 (m), 2021 (vs), 1995 (s), and 1950 (sh) cm^{-1} , along with a bridging carbonyl stretching band at 1892 (m) cm^{-1} . The vibrationally coupled $\nu(\text{CO})$ bands of the dione moiety appearing at 1716 (m) and 1684 (m) cm^{-1} are shifted some 33 cm^{-1} to lower frequency relative to the corresponding $\nu(\text{CO})$ bands in cluster **3** indicative of bpcd π bond coordination to a ruthenium center. The ^1H NMR spectrum of **4** exhibited an AB quartet centered at $\delta 3.54$ that is readily attributed to the methylene group of the bpcd ligand. No high-field hydride(s) resonance(s) was found, and this when coupled with the presence of only twenty-five aromatic hydrogens from $\delta 8.00\text{--}6.60$, supports the loss of a molecule of benzene in the formation of cluster **4**. The ^{31}P NMR spectrum showed the presence of three sets of resonances consisting of doublet of doublets centered at $\delta 249.97$, 64.60 , and 6.14 . The latter high-field resonance may be confidently assigned to the $\text{Ph}_2\text{P}(\text{dione})$ moiety, and the large coupling constant of 171 Hz indicates that this $\text{Ph}_2\text{P}(\text{dione})$ moiety is situated *trans* to the lowest field phosphido group at $\delta 249.97$. The unambiguous identity for these ^{31}P groups in cluster **4** and the phosphorus locus from which the benzene molecule originates were established by X-ray crystallography.

The ORTEP diagram shown in Fig. 2 confirms the molecular structure of cluster **4** and establishes the course of the ancillary bpcd ligand activation upon thermolysis. Cluster **4** contains 48 valence electrons and is isoelectronic relative to cluster **3**. The original bridging phosphido moiety, which is represented by the P(3) atom, has been regenerated through a reductive coupling of the C(312a) atom with one of the hydride ligands in $\text{H}_2\text{Ru}_3(\text{CO})_7(\text{bpcd})[\mu, \sigma\text{-PPh}(\text{C}_6\text{H}_4)]$, and the loss of a phenyl group from the bpcd ligand gives rise to the observed $7e\text{-donor}$ ligand $\mu, \eta^2, \eta^1\text{-PPhC}=\text{C}(\text{PPh}_2)\text{C}(\text{O})\text{CH}_2\text{C}(\text{O})$ that face caps the triruthenium frame via phosphido and phosphine moieties, and the C=C π bond of the dione ring. The departed phenyl group leaves as benzene presumably from a reductive elimination

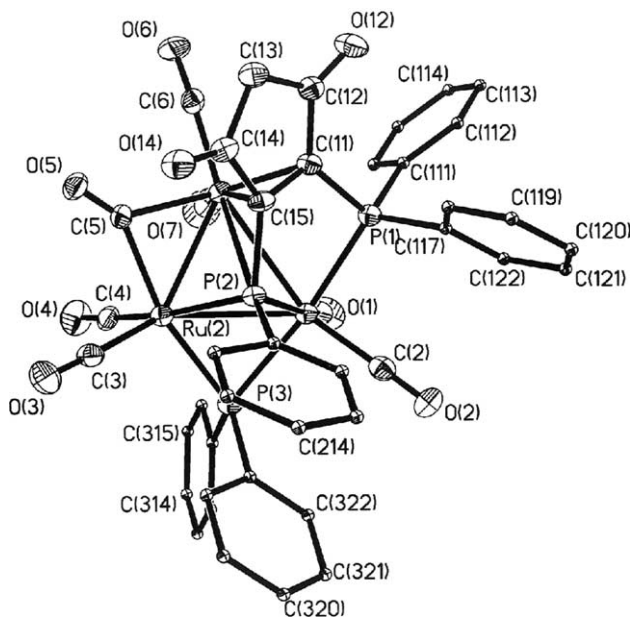


Fig. 2. ORTEP drawing of $\text{Ru}_3(\text{CO})_6(\mu\text{-CO})(\mu\text{-PPh}_2)[\mu,\eta^2,\eta^1\text{-PPhC}=\text{C}(\text{PPh}_2)\text{C}(\text{O})\text{CH}_2\text{C}(\text{O})]$ showing the thermal ellipsoids at the 50% probability level.

process involving a putative Ru–P moiety and the remaining hydride ligand [23]. The Ru–Ru bond lengths range from 2.742(1) Å [Ru(2)–Ru(3)] to 2.981(1) Å [Ru(1)–Ru(3)] and exhibit an average distance of 2.875 Å, consistent with their single-bond designation. The five distinct Ru–P bond distances display a mean distance of 2.347 Å and agree well with other reported Ru–P distances in polynuclear ruthenium clusters. The P(1)–Ru(1)–P(2), P(1)–Ru(1)–P(3), and P(2)–Ru(1)–P(3) groups show angles of 84.67(8)°, 164.86(6)°, and 80.22(8)°, respectively, and support the assignments of the ^{31}P NMR resonances for cluster **4**, namely, a tertiary phosphine group [$\text{Ph}_2\text{P}(\text{dione})$ moiety] that is *cis* to one phosphido group and *trans* to a second phosphido group. The bridging C(5)O(5) group that spans the Ru(2)–Ru(3) vector appears symmetrically bound based on Ru(2)–C(5) and Ru(3)–C(5) bond distances of 2.133(8) and 2.133(1) Å, respectively, and angles of 143.3(8)° and 136.0(8)° for the atoms Ru(2)–C(5)–O(5) and Ru(3)–C(5)–O(5), respectively. Coordination of the C(11)–C(15) bond to Ru(3) leads to a 0.08 Å elongation relative to the free π bond found in cluster **3**, consistent with the Duncanson–Dewar–Chatt model for the bonding between an alkene and a transition metal [24].

4. Conclusions

Coordination of the diphosphine ligand bpcd to the activated cluster $\text{HRu}_3(\text{CO})_9(\mu\text{-PPh}_2)$ (**2**) leads to the replacement of two CO ligands and facile orthometalation of one of the phenyl groups of the phosphido group

to furnish $\text{H}_2\text{Ru}_3(\text{CO})_7(\text{bpcd})[\mu,\sigma\text{-PPh}(\text{C}_6\text{H}_4)]$. The same product is also obtained from the saturated cluster $\text{HRu}_3(\text{CO})_{10}(\mu\text{-PPh}_2)$ upon thermolysis and Me_3NO activation. $\text{H}_2\text{Ru}_3(\text{CO})_7(\text{bpcd})[\mu,\sigma\text{-PPh}(\text{C}_6\text{H}_4)]$ is thermally unstable and transforms to $\text{Ru}_3(\text{CO})_6(\mu\text{-CO})(\mu\text{-PPh}_2)[\mu,\eta^2,\eta^1\text{-PPhC}=\text{C}(\text{PPh}_2)\text{C}(\text{O})\text{CH}_2\text{C}(\text{O})]$, as the net result of reversible orthometalation and P–Ph bond cleavage of the ancillary bpcd, followed by loss of benzene. Both product clusters have been isolated and fully characterized in solution and their molecular structures established by X-ray crystallography. Our future efforts will concentrate on determining the generality associated with the phosphine ligand induced orthometalation in the clusters $\text{HRu}_3(\text{CO})_{10}(\mu\text{-PPh}_2)$ and $\text{HRu}_3(\text{CO})_9(\mu\text{-PPh}_2)$.

5. Supplementary materials

Crystallographic data for the structural analyses have been deposited with the Cambridge Crystallographic Data Center, CCDC No. 264527 for **3** and 264526 for **4**. Copies of this information may be obtained free of charge from the Director, CCDC, 12 Union Road, Cambridge, CB2 1EZ UK [Fax: +44(1223)336-033; email: deposit@ccdc.ac.uk or <http://www.ccdc.cam.ac.uk>].

Acknowledgement

Financial support from the Robert A. Welch Foundation (B-1093-MGR) is appreciated.

References

- [1] S.A. MacLaughlin, N.J. Taylor, A.J. Carty, *Organometallics* 3 (1984) 392.
- [2] A.J. Carty, *Pure Appl. Chem.* 54 (1982) 113.
- [3] F.V. Gestel, S.A. MacLaughlin, M. Lynch, A.J. Carty, E. Sappa, A. Tiripicchio, M.T. Camellini, *J. Organomet. Chem.* 326 (1987) C65.
- [4] M. Castiglioni, R. Giordano, E. Sappa, *J. Organomet. Chem.* 362 (1989) 399; *J. Organomet. Chem.* 369 (1989) 419.
- [5] C. Allasia, M. Castiglioni, R. Giordano, E. Sappa, F. Verre, *J. Cluster Sci.* 11 (2000) 493.
- [6] (a) S.A. MacLaughlin, N.J. Taylor, A.J. Carty, *Inorg. Chem.* 22 (1983) 1411; (b) D. Nucciarone, S.A. MacLaughlin, A.J. Carty, *Inorg. Synth.* 26 (1989) 264.
- [7] S.A. MacLaughlin, A.J. Carty, N.J. Taylor, *Can. J. Chem.* 60 (1982) 87.
- [8] For an example of a related Fe_3 cluster possessing an η^2 tethered P–Ph bond and its reactivity with two-electron donor ligands, see: K. Knoll, G. Huttner, L. Zsolnai, O. Orama, M. Wasiucionek, *J. Organomet. Chem.* 310 (1986) 225.

- [9] M. Brookhart, M.L.H. Green, *J. Organomet. Chem.* 250 (1983) 395.
- [10] M. Lanfranchi, A. Tiripicchio, E. Sappa, A.J. Carty, *J. Chem. Soc., Dalton Trans.* (1986) 2737.
- [11] W.H. Watson, M.A. Mendez-Rojas, Y. Zhao, M.G. Richmond, *J. Chem. Crystallogr.* 33 (2003) 767.
- [12] (a) For other examples of metal cluster reactions with the bpcd ligand, see: H. Shen, S.G. Bott, M.G. Richmond, *Organometallics* 14 (1995) 4625;
(b) S.G. Bott, H. Shen, R.A. Senter, M.G. Richmond, *Organometallics* 22 (2003) 1953;
(c) S.G. Bott, H. Shen, M.G. Richmond, *J. Organomet. Chem.* 689 (2004) 3426.
- [13] M.I. Bruce, C.M. Jensen, N.L. Jones, *Inorg. Synth.* 26 (1989) 259.
- [14] (a) D. Fenske, H. Becher, *Chem. Ber.* 107 (1974) 117;
(b) D. Fenske, *Chem. Ber.* 112 (1979) 363.
- [15] D.F. Shriver, *The Manipulation of Air-sensitive Compounds*, McGraw-Hill, New York, 1969.
- [16] D. Dolphin, A. Wick, *Tabulation of Infrared Spectral Data*, Wiley-Interscience, New York, 1977.
- [17] (a) P.E. Garrou, *Chem. Rev.* 81 (1981) 229;
(b) M.G. Richmond, J.K. Kochi, *Organometallics* 6 (1987) 254.
- [18] H. Jungbluth, G. Süss-Fink, M.A. Pellinghelli, A. Tiripicchio, *Organometallics* 8 (1989) 925.
- [19] (a) Y. Chi, H.-F. Hsu, L.-K. Liu, S.-M. Peng, G.-H. Lee, *Organometallics* 11 (1992) 1763;
(b) M.I. Bruce, E. Horn, P.A. Humphrey, E.R.T. Tiekink, *J. Organomet. Chem.* 518 (1996) 121;
(c) R.D. Adams, B. Captain, W. Fu, M.D. Smith, *J. Organomet. Chem.* 651 (2002) 124.
- [20] (a) J.F. Corrigan, S. Doherty, N.J. Taylor, A.J. Carty, *J. Am. Chem. Soc.* 114 (1992) 7557;
(b) N. Lugan, J.-J. Bonnet, J.A. Ibers, *Organometallics* 7 (1988) 1538;
(c) F.F. de Biani, C. Graiff, G. Opromolla, G. Predieri, A. Tiripicchio, P. Zanello, *J. Organomet. Chem.* 637 (2001) 586;
(d) M.I. Bruce, G.N. Pain, C.A. Hughes, J.M. Patrick, B.W. Skelton, A.H. White, *J. Organomet. Chem.* 307 (1986) 343;
(e) R. Mason, A.I.M. Rae, *J. Chem. Soc. A* (1968) 778.
- [21] D.M.P. Mingos, D.J. Wales, *Introduction to Cluster Chemistry*, Prentice Hall, Englewood Cliffs, NJ, 1990.
- [22] (a) S.G. Bott, H. Shen, M.G. Richmond, *Struct. Chem.* 12 (2001) 237;
(b) S.G. Bott, H. Shen, M.G. Richmond, *J. Chem. Crystallogr.* 28 (1998) 385;
(c) S.G. Bott, J.C. Wang, H. Shen, M.G. Richmond, *J. Chem. Crystallogr.* 29 (1999) 391.
- [23] While the exact reaction sequence involving the reformation of the original μ_2 -PPh₂ moiety and the elimination of a phenyl group from the bpcd ligand as benzene cannot be ascertained at this juncture, we favor a scenario that proceeds through initial regeneration of the phosphido ligand.
- [24] T.A. Albright, J.K. Burdett, M.H. Whangbo, *Orbital Interactions in Chemistry*, Wiley, New York, 1985.